Eur. Phys. J. B **15**, 127–132 (2000)

THE EUROPEAN PHYSICAL JOURNAL B

EDP Sciences

Aggregation of non-bonding molecules in a rapidly growing gel

J.C. Lee[a]

Department of Physics and Astronomy, University of Southern Mississippi, Hattiesburg, MS 39406-5046, USA

Received 30 November 1999

Abstract. The aggregation of non-bonding molecules in a rapidly growing gel is studied under three different conditions by means of Molecular Dynamics simulations. The aggregation takes place even under the unfavorable condition when the non-bonding molecules constitute only a small fraction of the total. The results also show that the morphology of the growing domains is different depending on the concentration of the non-bonding molecules.

PACS. 61.41.+e Polymers, elastomers, and plastics – 64.60.Cn Order-disorder transformations; statistical mechanics of model systems – 64.75.+g Solubility, segregation, and mixing; phase separation

1 Introduction

Consider a homogeneous mixture of molecules of species α and β which has a normal phase diagram with an upper critical temperature. In the composition-temperature phase diagram, the system is at a point above the spinodal and binodal lines. There are several ways to phase separate such a mixture. The best known is to quench the temperature which induces the phase separation known as spinodal decomposition. If species β are monomers, phase separation may also be induced by polymerizing them [1–4]. If the polymerization rate is slow, the system point remains stationary, but the phase boundary lines (of molecules of species α and the growing polymers of species β) are gradually altered in shape and pushed up towards the system point, and phase separation occurs when they engulf the system point [2]. The nature of the instability against phase separation is therefore the same as in the temperature quench. There are two important time scales: $\tau_{\rm pl}$, the time scale for polymerization, and $\tau_{\rm ps}$, the time scale for phase separation. In order for the above polymerization-induced phase separation to occur, it is necessary that $\tau_{\rm pl} \gg \tau_{\rm ps}$.

What if the polymerization rate is very fast allowing little or no time for α molecules to aggregate? To make it even more difficult for α molecules to aggregate, what if the monomers form a cross-linked network of a gel trapping the non-bonding α molecules? The relationship between chemical reactions and pattern-forming ordering processes can be colorful. The two can be put in a competition, and the polymerization or other chemical reaction can be exploited to arrest a particular pattern of morphology or to manipulate a novel morphology [5]. In the present case, there is no competition; it is simply a question of whether the trapped α molecules will remain buried in the network or will conspire with the growing gel to escape the traps and aggregate. The first experiment involving such a system was performed by Serbutoviez *et al.* who used liquid crystal for non-bonding species α and TEGDA for monomers [6]. The liquid crystal molecules do aggregate to form droplets in the matrix of a gel. In this case, $\tau_{\rm pl} \ll \tau_{\rm ps}$.

We performed recently a Molecular Dynamics simulation with simple Lennard-Jones molecules for both α and β [7]. In this simulation, the majority of the β molecules are tri-functional (meaning that each can support a maximum of three bonds) and a small remainder bi-functional. The non-bonding α molecules aggregate following what appears to be a well defined dynamics; the droplets grow following a power law and the structure factor evolves following a dynamic scaling. We proposed the following explanation for the aggregation. When the network traps the non-bonding α molecules, it essentially freezes the positional entropy of α molecules. Should they overcome the barriers and aggregate to form droplets, the small bits of space available only to each of the trapped molecules would be turned into much larger pieces of space in which many α molecules can move around. The growing gel and the trapped α molecules do just that to increase the entropy. Nature abounds with entropy-driven ordering processes [8], but the present example is unique in that the entropy incentive is provided by energy barriers. Leave the $\alpha+\beta$ mixture alone, there will no aggregation. Try to trap the α molecules with energy barriers as if they had to be kept from aggregating, they will aggregate.

In the above simulation, however, the fraction of α and β are equal and therefore even before the polymerization begins there are already groups of α molecules in small clusters. Near such clusters the network is incomplete, which helps the clusters grow into droplets. If this is the main reason for the aggregation, there may not be

[a] e-mail: lee@otter.st.usm.edu

any aggregation in off-critical mixtures where the network is more complete and poses more rugged energy barriers. The purpose of this paper is to vary the network rigidity, or the degree of trapping power, and see how it affects the aggregation. To this end, we run MD simulations with three systems which have different degrees of network rigidity.

2 Model

The $\alpha-\alpha$ and $\beta-\beta$ pair interactions are both given by $4\epsilon\{(\sigma/r)^{12} - (\sigma/r)^6\}$, while the $\alpha-\beta$ pair interaction is given by $4\epsilon\{(\sigma/r)^{12} - 0.6(\sigma/r)^6\}$. The factor 0.6 weakens the attraction tail of the inter-species interaction and makes the phase diagram normal. To simplify the computation, we also assume that both species have the same mass m.

Some of the monomers (β molecules) are tri-functional while others are bi-functional. We adapt the method of Herrmann *et al.* [9] to model the radical addition polymerization process that uses UV. The photo polymerization is advantageous because the polymerization rate can be chosen independent of the temperature. To this end, a certain number of monomers are randomly chosen initially as active monomers; the fraction of the active monomers to the total determines the polymerization rate. If an active monomer comes within the prescribed distance $R_{\min}$ of another monomer which has at least one functionality left, a bond is formed between the two. If the latter was not active before the encounter, it now becomes active while the initial active monomer becomes inactive. If both were active, on the other hand, both become inactive after the reaction. As the polymerization progresses, there are not enough active monomers left and those still remaining active are at wrong places. Thus we periodically activate more monomers. We choose $R_{\min} = 0.9\sigma$.

The bond is represented by the FENE potential:

$$\phi(r) = \begin{cases} -0.5KR_0^2 \ln(1-(r/R_0)^2) & r \le R_0 \\ 0 & r \ge R_0 \end{cases}$$

where R_0 represents the maximum elongation that the bond can suffer. We choose: $K = 30.0\epsilon/\sigma^2$, $R_0 = 1.5\sigma$.

A total of $N = 7500$ molecules are placed in a self-closed slab (with periodic boundary conditions) of $L_x \times L_y \times L_z$, where $L_x = L_y \equiv L = 50\sigma$, and $L_z = 3\sigma$; the density is $0.85/\sigma^3$. The details of the mixture composition will be given when each system is introduced later. The molecular positions and velocities are updated for each time increment of $\delta t = 0.004$ in the time units of $\tau = (m\sigma^2/48\epsilon)^{1/2}$. From now, what we will call time t is the unitless reduced time *i.e.*, t/τ.

As the polymerization proceeds, we measure at various times the equal-time structure factor

$$S(q,t) = \langle \rho(q,t)\rho(-q,t)\rangle/2N,$$

where t is the elapsed time from the moment the polymerization began. We write the concentration fluctuation $\rho(q,t)$ in the form of

$$\rho(q,t) = \sum_{\alpha i} \exp(\mathrm{i}\mathbf{q}\cdot\mathbf{r}_{\alpha i}) - \sum_{\beta i} \exp(\mathrm{i}\mathbf{q}\cdot\mathbf{r}_{\beta i}),$$

where the negative sign in the second term provides a dielectric contrast between the two species. The probed wave vectors are: $q = 2\pi k/L$ where $k = 1, 2, 3, 4, ...\, 18$. For each k, we probe the fluctuations in the x direction and y direction, and then take the average. For the ensemble average, many runs are repeated with different initial configurations; the ensemble size varies between 41 and 51.

3 Results and discussion

In order to study the effect of the network rigidity on the aggregation, we introduce three different systems. A factor pertinent to the network rigidity is the number of bonds. In the bond-forming process, the non-bonding α molecules are not just a bystander. Since bonds cannot be formed if an α molecule is in the way, they in fact dictate the process. Another factor that affects the network rigidity is the fraction of the bi-functional monomers; the more bi-functional monomers, the more flexibility. With these two factors in mind, we introduce systems I, II and III. System I is the same as studied previously [7] except that the bonds are not allowed to break. It serves as the reference system with which systems II and III are to be compared. Among the three, the network is most rigid in system II and least rigid in system III.

(i) System I

The mixture has α and β molecules at equal proportion. Among the monomers (β molecules), approximately 97 percent are tri-functional and 3 percent bi-functional. The initial fraction of the active monomers is 34.3 percents, which makes the gelation very fast. The results for the structure factor are shown in Figure 1, and the peak position movement in Figure 2. Figure 3 shows the scaling plot, $S(k,t)/S(k_{\mathrm{m}},t)$ *vs.* k/k_{m}, where k_{m} represents the peak position. In the scaling region which begins approximately at $t = 60$, the growth follows $k_{\mathrm{m}}(t) \sim t^{-a}$, with $a = 0.26$.

(ii) System II

System II is the same as system I except that the initial mixture is off-critical with more monomers than α molecules at the ratio of 7 to 3. The results are shown in Figures 4 and 5. Since most of the α molecules are individually hidden in the sea of monomers, their paths to droplets are truly rugged and long. The odd of finding droplets under such a condition may appear poor, but the results leave no doubt that the α molecules do aggregate. The details of the dynamics are, however, difficult to study. In the ordinary nucleation and growth, the growth is driven by the local imbalance of chemical potential. That is not the case here. An α molecule can be

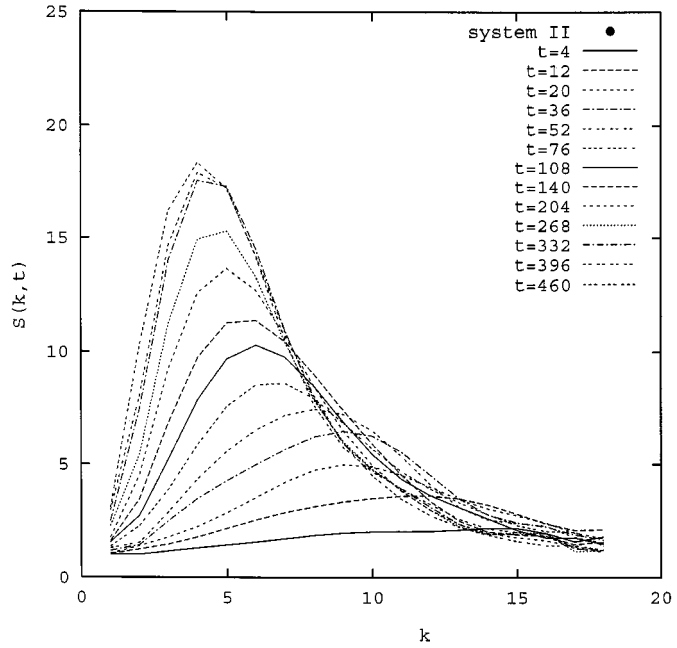

Fig. 1. The equal-time structure factor $S(k,t)$ of system I plotted *vs.* k.

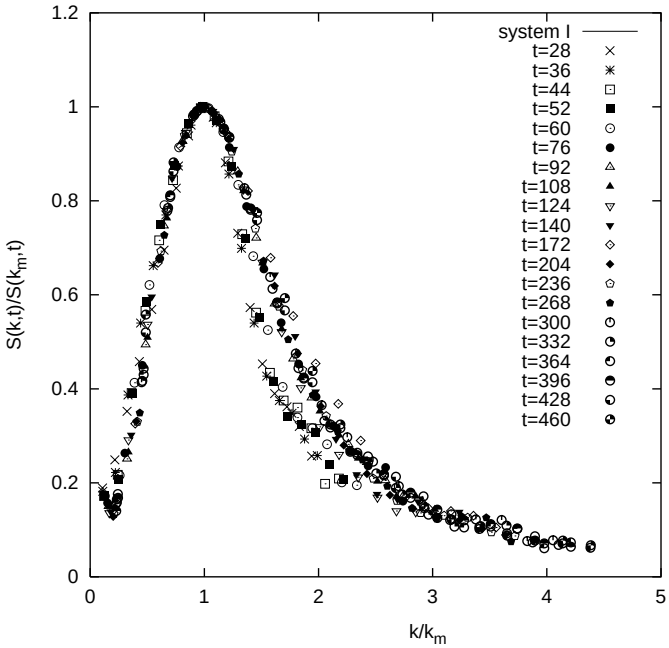

Fig. 3. The scaled structure factor plotted *vs.* the scaled wave vector for system I.

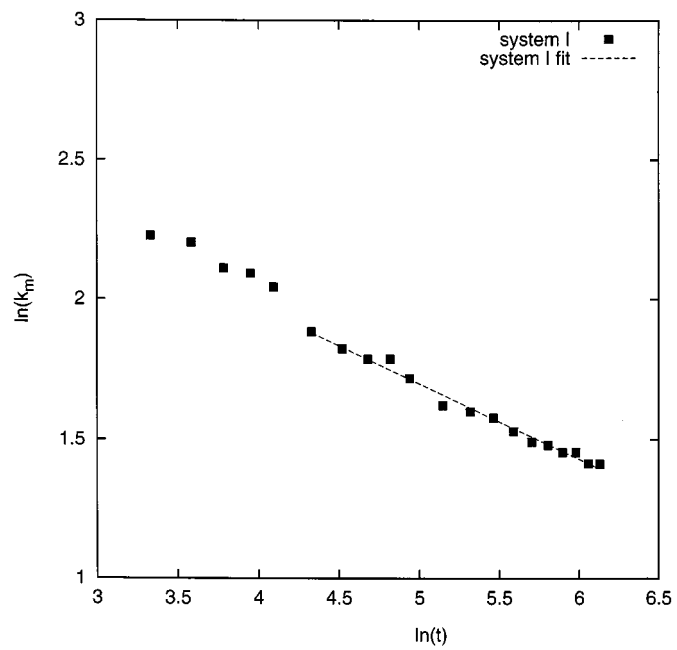

Fig. 2. Log-log plot of the peak position $k_{\rm m}(t)$ *vs.* time t for system I.

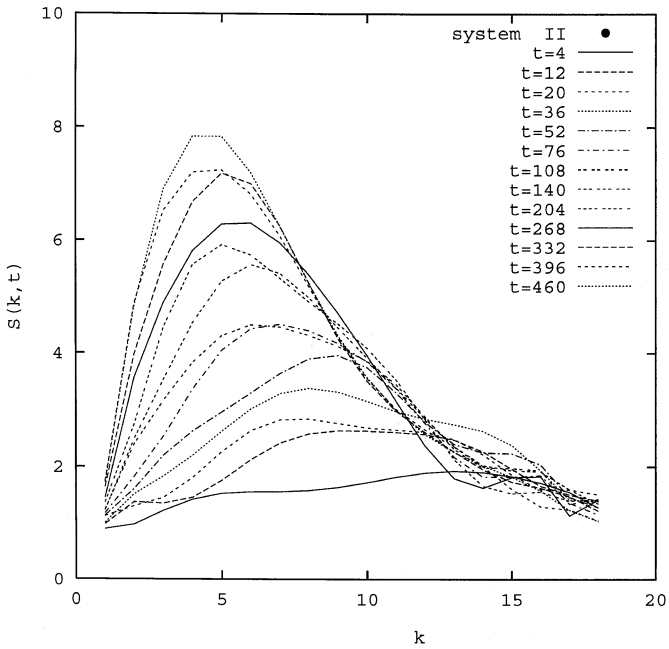

Fig. 4. The equal-time structure factor $S(k,t)$ of system II plotted *vs.* k.

trapped in the immediate vicinity of a droplet, but there is no guarantee that it will go to the nearby droplet. Depending on the surrounding energy landscape that it has to go through, it could ultimately arrive at the nearby droplet or one very far away. Due to this randomness, the fluctuation from one sample (in the ensemble) to another is very large, and calls for a very large ensemble for a reliable average.

Although the ensemble size 51 is the largest among the three systems, it is not large enough and there is a considerable degree of uncertainty. With this proviso, the most prominent in Figure 5 is the oscillation. It is not clear to what extent it is a result of the insufficient ensemble size. Figure 6 shows the scaling plot. The scaled data are scattered over a wide range, but the scatter is more or less random, which we take as suggesting that the scaling actually holds and the oscillation in Figure 5

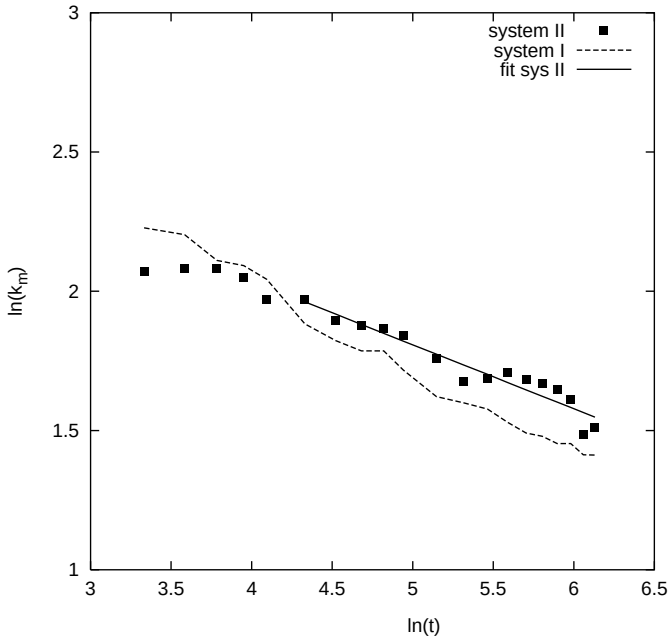

Fig. 5. Log-log plot of the peak position $k_{\rm m}(t)$ *vs.* time t for system II. The corresponding result of system I is also shown for comparison.

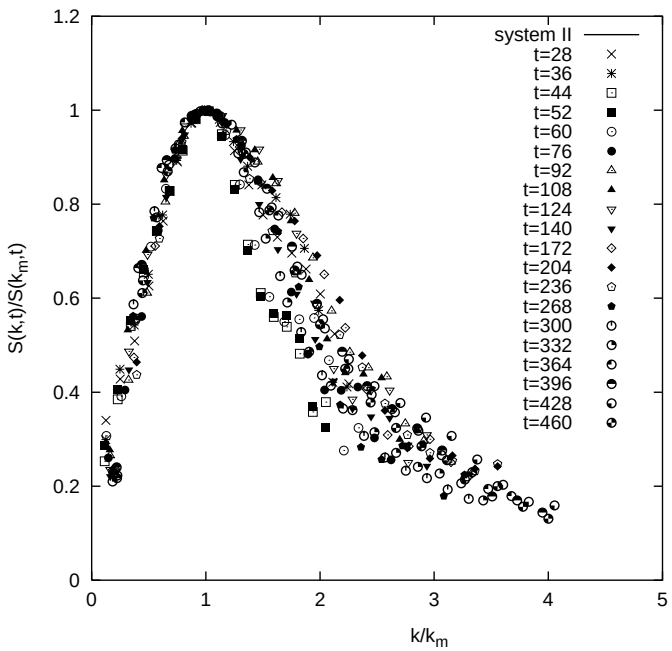

Fig. 6. The scaled structure factor plotted *vs.* the scaled wave vector for system II.

is an artifact of the insufficient ensemble size. On that assumption, if we fit the last fifteen data points in Figure 5, the growth exponent a is approximately 0.23. Figure 7 compares system I and II in terms of their scaled structure factors. Although our data are not accurate enough to display the scaling function of system II, the data are accurate enough to show that it is different from that of system I. Figures 8 and 9 show the molecular morphology

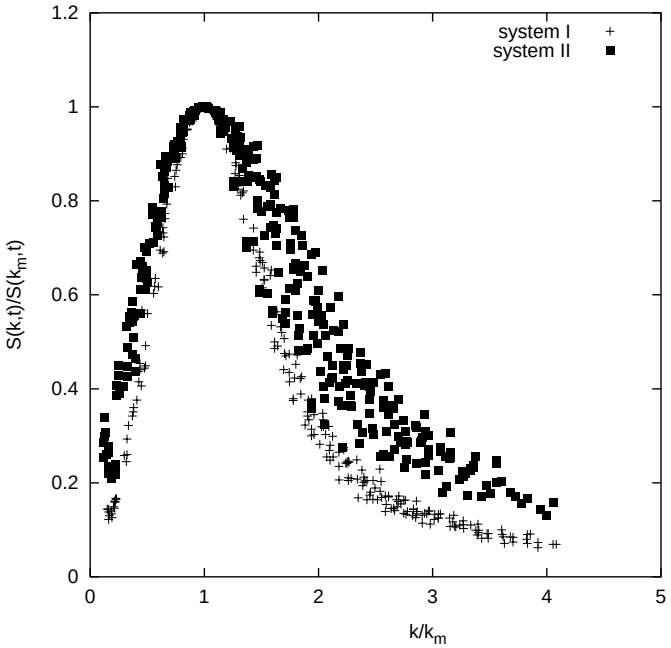

Fig. 7. Comparison of the scaled structure factors of system I and system II.

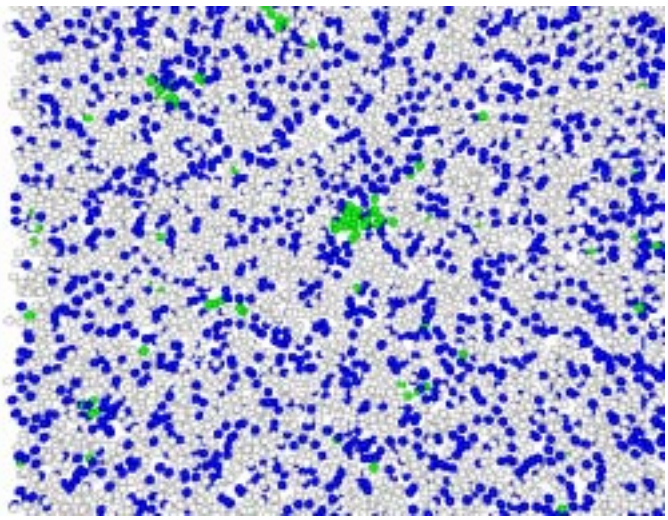

Fig. 8. The molecules of system II at $t = 4$. The dark shade represents α molecules, the light shade those monomers that have joined the spanning gel, and the intermediate shade those monomers that have not joined yet.

at $t = 4$ and $t = 460$, respectively. It is noticeable that at $t = 4$ there is already a spanning gel.

(iii) System III

System III is the same as system I except that the mixture has more bi-functional monomers than tri-functional monomers by the ratio of 3 to 2. This makes the gel network more flexible. The results are shown in Figures 10 and 11. The scarcity of the tri-functional monomers results in an inhomogeneous network structure; there are regions unusually rich in the tri-functional monomers here and

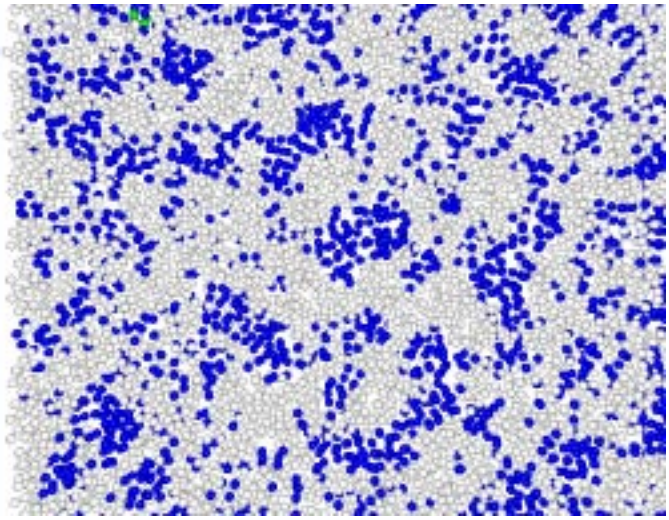

Fig. 9. The molecules of system II at $t = 460$. The dark shade represents α molecules, the light shade those monomers that have joined the spanning gel, and the intermediate shade those monomers that have not joined yet.

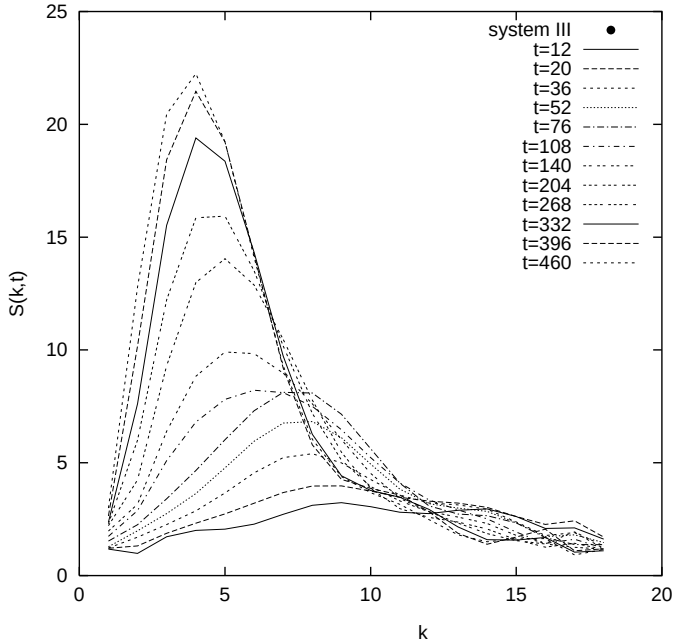

Fig. 10. The equal-time structure factor $S(k,t)$ of system III plotted *vs.* k.

there. This again calls for a large ensemble, and results in numerical uncertainty. The peak position hardly changes at early times, but starting from about $t = 108$ it moves following a power law pattern with the growth exponent $a = 0.32$. The late entrance into the power-law regime and the increased growth exponent are both consistent with the entropy argument. Due to the scarcity of the tri-functional monomers, polymerization only yields disjoint chains at early times. It is therefore difficult to trap α molecules, which is the reason for the late arrival of the power law regime. The network does trap α molecules at late times when the chains are adequately cross-linked but

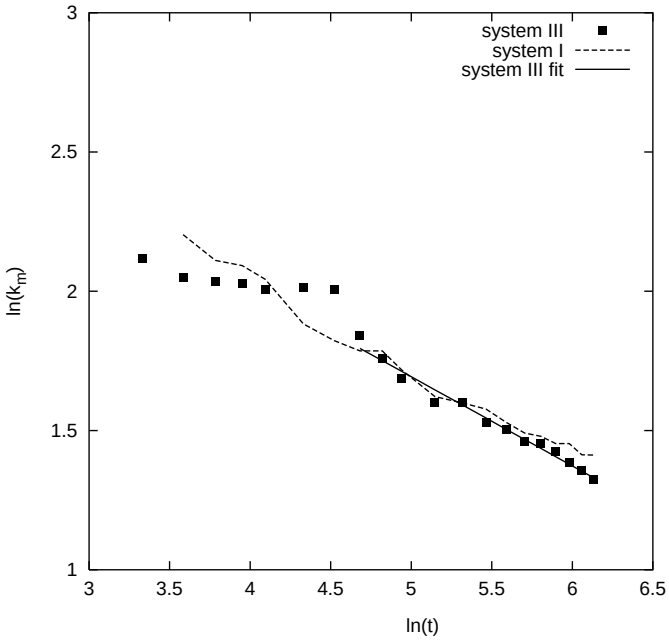

Fig. 11. Log-log plot of the peak position $k_{\rm m}(t)$ *vs.* time t for system III. The corresponding result of system I is also shown for comparison.

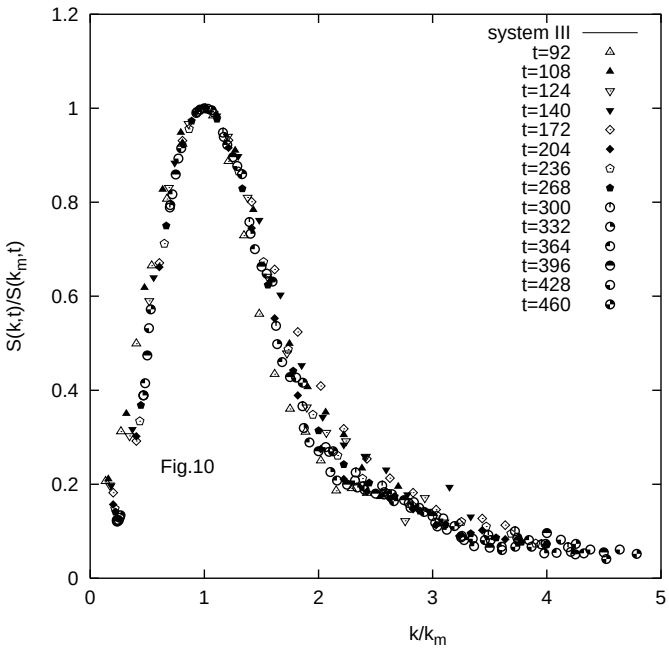

Fig. 12. The scaled structure factor plotted *vs.* the scaled wave vector for system III.

still not with as much barriers as in system I, which is the reason for the increased growth exponent. We estimate the growth exponent to be $a = 0.32$, a number close to what a would be in a diffusion-limited growth after a temperature quench.

The scaling plot for the late time regime is shown in Figure 12 and is compared with that of system I in

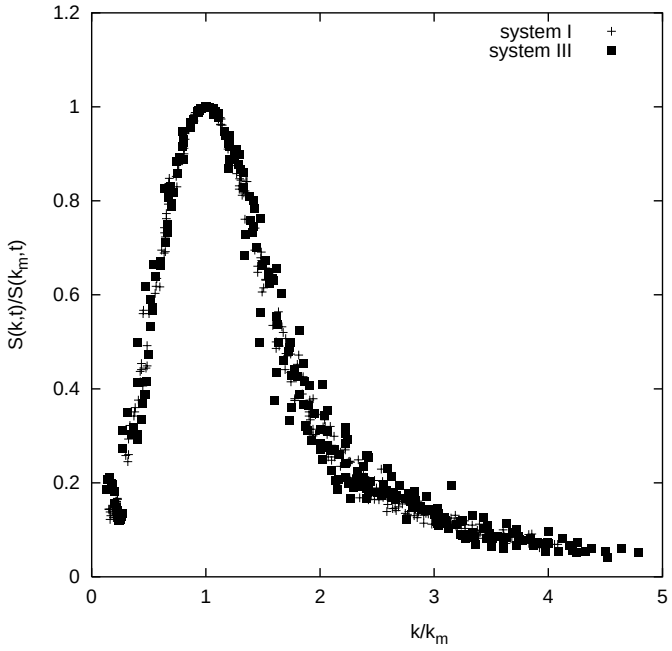

Fig. 13. Comparison of the scaled structure factors of system I and system III.

Figure 13. The two scaling functions are the same within the uncertainty.

To conclude, we have studied three different systems. System III is different from system I in terms of the network flexibility, but are the same in terms of the fraction of the non-bonding molecules. System II is different from system I on both accounts. The fact that system I shares the same scaling function with system III but not with system II suggests that the domain morphology is different depending on the fraction of the non-bonding molecules. The system that Serbutoviez *et al.* studied is much more complex than ours, but they also observe the same result: the morphology of the liquid-crystal rich domains is different depending on the concentration of the liquid-crystal component. In the meantime, the growth exponent decreases with increasing degree of network rigidity, as anticipated.

This work was initiated as a simplified model of PDLC (polymer dispersed liquid crystal)-forming process in which the molecules of species β are liquid crystal. For such systems, the dynamics of the droplet growth is not well understood when the polymerization rate is fast, which motivated the simulation. The dynamics is better understood for slow polymerization, but there are issues waiting for further study [3].

Thus in our next report we will investigate how the polymerization rate affects the dynamics. The dynamics in an already-formed gel has been studied by various authors [10]. We will hope to address this issue as well but with liquid crystal as the β component.

This research was supported by the Air Force Office of Scientific Research through DEPSCoR program.

References

1. J.Y. Kim, C.H. Cho, P. Palffy-Muhoray, M. Mustafa, T. Kyu, Phys. Rev. Lett. **71**, 2232 (1993).
2. J.-C. Lin, P.L. Taylor, Mol. Cryst. Liq. Cryst. **237**, 25 (1993).
3. G. Golemme, A. Urso, B.C. De Simone, A. Mashin, G. Chidichimo, Liq. Cryst. **24**, 563 (1998).
4. T. Kyu, J.-H. Lee, Phys. Rev. Lett. **76**, 3746 (1996).
5. H. Tanaka, T. Suzuki, T. Hayashi, T. Nishi, Macromolecules **25**, 4453 (1992); S. Glotzer, D. Stauffer, N. Jan, Phys. Rev. Lett. **72**, 4109 (1994); H. Furukawa, J. Phys. Soc. Jpn **63**, 3744 (1994). A. Imagawa, Q. Tran-Cong, Macromolecules **28**, 8388 (1995).
6. C. Serbutoviez, J.G. Kloosterboer, H.M. Boots, F.J. Touwslager, Macromolecules **29**, 7690 (1996).
7. J.C. Lee, Phys. Rev. E **60**, 1930 (1999).
8. See, for example, A.P. Gast, W.B. Russel, Phys. Tod. **51** (12), 24 (1998); M. Adams, Z. Dogic, S.L. Keller, S. Fraden, Nature **393**, 349 (1998).
9. H.J. Herrmann, D. Stauffer, D.P. Landau, J. Phys. A **16**, 1221 (1983).
10. See, for example, A.E. Bailey, B.J. Frisken, D.S. Cannell, Phys. Rev. E **56**, 3112 (1997); D. Stauffer, R.B. Pandey, J. Phys. A **25**, L1079 (1992); J.C. Lee, J. Chem. Phys. **110**, 8742 (1999).